Design of Organic Solar Cells as a Function of Radiative Quantum Efficiency

Blaise Godefroid* and Gregory Kozyreff†

Optique Nonlinéaire Théorique, Université libre de Bruxelles (ULB), CP 231, B-1050 Bruxelles, Belgium

(Received 23 May 2017; published 25 September 2017)

We study the radiative decay, or fluorescence, of excitons in organic solar cells as a function of its geometrical parameters. Contrary to their nonradiative counterpart, fluorescence losses strongly depend on the environment. By properly tuning the thicknesses of the buffer layers between the active regions of the cell and the electrodes, the exciton lifetime and, hence, the exciton diffusion length can be increased. The importance of this phenomenon depends on the radiative quantum efficiency, which is the fraction of the exciton decay that is intrinsically due to fluorescence. Besides this effect, interferences within the cell control the efficiency of sunlight injection into the active layers. The optimal cell design must rely on a consideration of these two aspects. By properly managing fluorescence losses, one can significantly improve the cell performance. To demonstrate this fact, we use realistic material parameters inspired from literature data and obtain an increase of power-conversion efficiency from 11.3% to 12.7%. Conversely, not to take into account the strong dependence of fluorescence on the environment may lead to a suboptimal cell design and a degradation of cell performance. The presence of radiative losses, however small, significantly changes the optimal set of thicknesses. We illustrate the latter situation with experimental material data.

DOI: 10.1103/PhysRevApplied.8.034024

I. INTRODUCTION

Organic solar cells attract considerable research interest as a low-cost, mechanically flexible, and low-temperature manufactured alternative to inorganic solar cells. Various architectures exist, including donor-acceptor bilayer heterojunctions [1], bulk heterojunctions [2], tandem structures [3], and cascaded exciton-dissociating heterojunctions [4]. One of the main factors that limits the efficiency of organic solar cells is the short diffusion length of excitons compared to the absorption length [5–7]. Indeed, because of the poor transport of photogenerated electrical excitations, the active layers are restricted to thicknesses that are too thin to fully absorb the incident sunlight. In order to overcome this difficulty, several photonic strategies have been devised to efficiently trap light: randomly structured interfaces [8], hexagonal arrays of nanocolums [9,10], nanoholes [11], and nanospheres [12,13]. More recently, a photonic fiber plate was shown to significantly improve light trapping through intermittent ray chaos [14,15]. While bulk heterojunctions are an answer to the exciton-transport problem, they come with additional difficulties, such as dead ends in the path of electrons and holes towards their respective electrodes and chemical stability. Moreover, nonradiative recombinations at interfaces between the donor and the acceptor are found to severely limit the efficiency of bulk-heterojunction cells [16,17]. Hence, bulk heterojunctions are not a definitive solution to exciton transport, and to increase the diffusion length of excitons in planar solar cells remains a critical objective.

Aside from material engineering, it has been pointed out that radiative losses (i.e., the diffusion length) can be optically engineered through the geometrical arrangement of the cell when it is thin and hence present microcavity effects [18]. Indeed, a radiating exciton is electromagnetically equivalent to an oscillating dipole. The optical power emitted by such a dipole can be increased or decreased in the proximity of boundaries, as was experimentally demonstrated by Drexhage [19]. A theoretical treatment of this radiation problem was worked out as early as 1909 by Sommerfeld in his study of antennas [20,21]. More-complete accounts followed Drexhage's pioneering experiments, both theoretically [22–25] and experimentally [26,27]. In high-Q cavities, it is well known that spontaneous emission of radiation can be strongly suppressed [28]. As for solar cells, they are, by construction, poor cavities, in order to let as much light in as possible. Nevertheless, it was found that spontaneous emission, i.e., radiative losses, can still be significantly reduced. A general rule to promote this effect is to sandwich the photoactive layer with low-index regions. Specifically, taking n_1 and n_2 as the refractive indexes of the active layer and its surrounding layer, respectively, the rate of spontaneous emission can be reduced by up to a factor of $(n_2/n_1)^5$ for excitons with a perpendicular orientation [18]. In addition to the above aspect, it has been emphasized that a proper choice of layer thickness inside the solar cell can significantly influence the distribution of sunlight intensity within the

*blaise.godefroid@ulb.ac.be
†gkozyref@ulb.ac.be

cell and, hence, the absorption of solar photon by the photoactive material [29–37].

The influence of exciton radiative losses on the device performance depends on the radiative quantum efficiency q, defined as

$$q = \frac{\Gamma_{\mathrm{r,bulk}}}{\Gamma_{\mathrm{bulk}}}, \qquad \Gamma_{\mathrm{bulk}} = \Gamma_{\mathrm{r,bulk}} + \Gamma_{\mathrm{nr}}, \tag{1}$$

where $\Gamma_{\mathrm{r,bulk}}$ and Γ_{nr} are the rate of radiative and nonradiative decay, respectively, and the "bulk" subscript indicates that it is the bulk value. The factor q is also called "fluorescence quantum efficiency" or "photoluminescence quantum efficiency." The bulk value of the radiative losses is an intrinsic quantity which is obtained in the absence of boundary effects. In a confined environment such as in an organic cell, the actual radiative losses $\Gamma_{\mathrm{r}}(z)$ generally differ from $\Gamma_{\mathrm{r,bulk}}$ and depend on the position, z, of the exciton. The total losses can be written as

$$\Gamma(z,q) = \Gamma_{\mathrm{bulk}}\left(1 - q + q\frac{\Gamma_{\mathrm{r}}(z)}{\Gamma_{\mathrm{r,bulk}}}\right). \tag{2}$$

In this paper, we seek to optimize the solar-cell geometry by taking both issues into account: efficient interference for sunlight absorption together with low exciton radiative losses. The fact that it is possible to reduce exciton emission while still efficiently admitting light into the solar cell relies on two observations: The exciton emits light (i) at a well-defined frequency, and (ii) in all directions. Conversely, sunlight comes in a broad spectrum and enters the cell through a narrow cone around the normal direction. In Ref. [18], only the short-circuit current was evaluated, and a simplified incident spectrum was assumed, which did not allow for evaluation of the cell power-conversion efficiency under a realistic illumination.

In order to assess device performance, we first establish a generalization of the Shockley-Queisser (SQ) theory [38] for organic solar cells. Indeed, in this classic theory, the transport of electrical excitations is not an issue since only inorganic semiconductor materials with high charge mobilities are considered. Besides, microcavity effects are absent from SQ theory. We therefore generalize SQ theory to take into account the diffusive exciton transport and microcavity effects for both sunlight injection and exciton radiation. In this more general theory, the external quantum efficiency (EQE), defined as the number of electrons generated per incoming photon, essentially replaces the material absorptivity.

The rest of the paper is organized as follows. In Sec. II, we present the generalized SQ theory, taking into account exciton transport with space-dependent radiative losses. In Sec. III, we apply our theory to several cell geometries and discuss the impact of q on the optimal cell design. Finally, we conclude.

II. GENERALIZED SHOCKLEY-QUEISSER THEORY

A. Shockly-Queisser detailed balance theory for conventional solar cells

In its simplest form, the SQ theory of solar cells derives from the following statement of detailed balance:

$$I_s = I_R(V) + I(V). \tag{3}$$

Above, I_s is the number of electron-hole (e-h) pairs generated per unit of time and area by photon absorption. From this current, a portion $I_R(V)$ will recombine to produce thermal electromagnetic radiation, leaving a particle current $I(V)$ [and hence an electrical current $-eI(V)$] of electrons to flow in the external circuit under an electrical potential V. For the sake of the present discussion, nonradiative recombination processes are omitted from the right-hand side of Eq. (3).

If each absorbed photon leads to the generation of one and only one electron-hole pair, then

$$I_s = \Omega_s \int_0^\infty a(\lambda)\phi_{\mathrm{AM1.5}}(\lambda)d\lambda, \tag{4}$$

where $\Omega_s = 6.85 \times 10^{-5}$ is the solid angle under which illumination is received from the Sun, $a(\lambda)$ is the absorptivity, $\phi_{\mathrm{AM1.5}}$ is the AM1.5 solar spectrum (in photons $\mathrm{s^{-1}\,m^{-2}\,m^{-1}\,sr^{-1}}$), and λ is the optical wavelength. We restrict our attention to illumination at normal incidence. Similarly, the recombination term is given by

$$I_R(V) = 2\pi \int_0^{\pi/2} \sin\theta\cos\theta \int_0^\infty a(\lambda)\phi(\lambda,T,V)d\lambda d\theta, \tag{5}$$

$$\phi(\lambda,T,V) = (2c/\lambda^4)\left[\exp\left(\frac{hc/\lambda - eV}{kT}\right) - 1\right]^{-1}. \tag{6}$$

Above, $\phi(\lambda,T,V)$ is the Planck's distribution in which the chemical potential of radiation is given by eV [39–41], c is the speed of light, h is Planck's constant, k is Boltzmann's constant, and T is the cell temperature. In Eq. (5), we use Kirchhoff's law and equate the emissivity of the cell with its absorptivity. Thus, Eq. (3) becomes

$$I(V) = \int_0^\infty a(\lambda)[\Omega_s\phi_{\mathrm{AM1.5}}(\lambda) - \pi\phi(\lambda,T,qV)]d\lambda. \tag{7}$$

This equation eventually leads to the Shockley-Queisser limit if we assume that $a(\lambda)$ is a step function. Stated in the above way, SQ theory can simply be generalized to a more general cell, such as those in which the internal electrical transport is controlled by excitons.

B. Exciton-regulated solar cell

In organic solar cells, the absorption of a photon gives rise to an exciton, with a binding energy that is large compared to kT. The excitons are therefore long-lived; moreover, being electrically neutral, their motion is governed by diffusion. It is only at the interface between the donor and acceptor materials that the local electric gradient can break the exciton into a free hole and a free electron. Neglecting other processes, elecron-hole pairs are generated by exciton dissociation only at the donor-acceptor interface, and they subsequently disappear only by radiative recombination or by being collected in the external circuit. Thus, the detailed-balance equation (3) becomes

$$I_\chi(\phi_{\mathrm{AM1.5}}) = I(V) + I_R(V), \tag{8}$$

where $I_\chi(\phi_{\mathrm{AM1.5}})$ is the exciton-dissociation current under the AM1.5 illumination equal to the number of e-h pair generated per unit of time and area. This term is independent of voltage since excitons are neutral particles. It can be expressed as

$$I_\chi(\phi_{\mathrm{AM1.5}}) = \Omega_s \int_0^\infty \mathrm{EQE}(\lambda, 0)\phi_{\mathrm{AM1.5}}(\lambda)d\lambda, \tag{9}$$

where we define $\mathrm{EQE}(\lambda,\theta)$ as the number of e-h pairs generated per incident photon with wavelength λ and incidence angle θ with respect to the normal direction. This coincides with the usual definition if the charge-collection efficiency is unity at short circuit, which is a common assumption [29,42].

Next, we must establish the radiative current $I_R(V)$. We first note that, in the dark, under an ambient isotropic illumination, $\phi(\lambda, T, 0)$, it must be equal to the e-h generation current, I_χ, as equilibrium conditions request.

$$I_R(0) = 2\pi \int_0^{\pi/2} \sin\theta\cos\theta \int_0^\infty \mathrm{EQE}(\lambda,\theta)\phi(\lambda, T, 0)d\lambda d\theta. \tag{10}$$

Outside equilibrium, the cell emits light with a potential of radiation, as in Eq. (6). In that case, one postulates that Eq. (10) can be extrapolated to nonzero values of V as

$$I_R(V) = 2\pi \int_0^{\pi/2} \sin\theta\cos\theta \int_0^\infty \mathrm{EQE}(\lambda,\theta)\phi(\lambda, T, V)d\lambda d\theta. \tag{11}$$

The validity of this modeling step is discussed and confirmed in Ref. [43]. Note that this last expression is similar to Eq. (5) but with the absorptivity, $a(\lambda)$, replaced by $\mathrm{EQE}(\lambda,\theta)$ [44]. Finally, Eq. (8) yields

$$\begin{aligned} I(V) = \Omega_s &\int_0^\infty \mathrm{EQE}(\lambda, 0)\phi_{\mathrm{AM1.5}}(\lambda)d\lambda \\ &- 2\pi \int_0^{\pi/2} \sin\theta\cos\theta \\ &\times \int_0^\infty \mathrm{EQE}(\lambda,\theta)\phi(\lambda, T, V)d\lambda d\theta. \end{aligned} \tag{12}$$

A similar derivation can be found in Refs. [45,46]. Other phenomenological factors, such as series and parallel resistances and the ideality factor, are unnecessary for the present discussion and are therefore omitted from the model. Note that the theory so far is very general and is valid beyond the theory of organic cells. In order to determine the current-voltage curve (12) for a given cell, one has to calculate $\mathrm{EQE}(\lambda,\theta)$. This is what we do in the next section for bilayer-heterojunction organic solar cells.

C. Calculation of EQE

We now wish to compute $\mathrm{EQE}(\lambda,\theta)$, i.e., the number of e-h pairs produced at the donor-acceptor interface per incoming photon as a function of the photon wavelength and incidence angle.

Let $N(\lambda,\theta) = \phi_{\mathrm{AM1.5}}(\lambda)\cos\theta$ be the number of photons that are incident per unit time and device area at an angle θ. This illumination results in an electromagnetic intensity distribution $g(z,\lambda,\theta)$ inside the device, which can be computed by the transfer-matrix method [47,48] (with unpolarized light assumed). With the proper normalization for $g(z,\lambda,\theta)$, which takes into account the absorption coefficient and the conversion efficiency of absorbed photons into excitons, the rate of production of excitons per unit length is $N(\lambda,\theta)g(z,\lambda,\theta)$. Hence, the distribution of excitons ρ produced by the flux $N(\lambda,\theta)$ satisfies

$$D\frac{\partial^2\rho}{\partial z^2} - \Gamma(z,q)\rho + N(\lambda,\theta)g(z,\lambda,\theta) = 0, \tag{13}$$

with

$$\frac{\partial\rho}{\partial z} = 0, \qquad z = z_{-1}, \tag{14a}$$

$$\rho = 0, \qquad z = z_0, \tag{14b}$$

$$\frac{\partial\rho}{\partial z} = 0, \qquad z = z_1. \tag{14c}$$

Above, D is the exciton diffusion constant, which takes the value D_A or D_D in the acceptor or donor material, respectively. Next, $\Gamma(z,q)$ is the exciton decay rate, which is computed as in Ref. [18] assuming random exciton orientation. Finally, Eq. (14) expresses a no-flux boundary condition for excitons at the interfaces ($z = z_{\pm 1}$) between the active layers and the adjacent blocking layers, while $\rho(z_0) = 0$ models complete exciton dissociation into free

electrons and holes at the donor-acceptor interface [29,42,49]. Exciton dissociation into free electrons and holes is assumed to be negligible everywhere else [50].

Note that if we divide Eq. (13) by Γ_{bulk} and normalize ρ as $\rho = (N/\Gamma_{\text{bulk}})\rho'$, the exciton-transport equation becomes

$$L^2 \frac{\partial^2 \rho'}{\partial z^2} - \frac{\Gamma(z,q)}{\Gamma_{\text{bulk}}}\rho' + g(z,\lambda,\theta) = 0, \qquad L^2 = \frac{D}{\Gamma_{\text{bulk}}}. \tag{15}$$

Solving that equation, the diffusive current at the donor-acceptor interface yields the EQE as

$$\begin{aligned}\text{EQE}(\lambda,\theta) &= \frac{1}{N(\lambda)}\left(D_D \left.\frac{\partial \rho}{\partial z}\right|_{z_0+\epsilon} - D_A \left.\frac{\partial \rho}{\partial z}\right|_{z_0-\epsilon}\right) \\ &= L_D^2 \left.\frac{\partial \rho'}{\partial z}\right|_{z_0+\epsilon} - L_A^2 \left.\frac{\partial \rho'}{\partial z}\right|_{z_0-\epsilon}. \end{aligned} \tag{16}$$

Once $\text{EQE}(\lambda,\theta)$ is determined, the $I(V)$ curve and the power-conversion efficiency can be computed from Eq. (12).

III. NUMERICAL RESULTS

In this section, we illustrate our theory with two bilayer cells, each one of the form Ag/HBL(h_b)/acceptor/donor/EBL(h_t)/ITO/glass. Here, Ag designates the back silver electrode, HBL is a hole-blocking and electron-transporting layer with thickness h_b, and EBL is an electron-blocking and hole-transporting layer with thickness h_t. Finally, ITO denotes a transparent indium tin oxide electrode (ultrathin metal film could be considered instead [37,51], but we omit this possibility here, as doing so does not change our general conclusions).

Given the large number of geometrical parameters available, we choose to maximize the cell power-conversion efficiency by varying only the thickness h_b and h_t of the HBL and EBL, respectively, for a given q. These two thicknesses are easily tunable fabrication parameters and it has been pointed out that they can significantly affect the efficiency of the cell [29–37].

As we vary q, we keep the bulk diffusion length unchanged, so as to compare active regions that would otherwise be equivalent. The power-conversion efficiency is given by

$$\eta = \max_V[-eI(V)V]/\Omega_s \int_0^\infty (hc/\lambda)\phi_{\text{AM1.5}}(\lambda)d\lambda. \tag{17}$$

We consider two distinct situations. First, we demonstrate the potential benefit of using large-q photoactive organic molecules if the cell is properly designed. To this end, we assume a favorable set of refractive indexes and thicknesses within ranges that are dictated by the literature. We show that a substantial gain in cell efficiency can be obtained.

Second, we simulate the following cell: Al/BCP/C_{70}/DBP/MoO_3/ITO/glass, for which we use experimentally measured refractive indexes. Here, BCP stands for bathocuproine and DBP for tetraphenyldibenzoperiflanthene. The photovoltaic junction is achieved by C_{70} (acceptor) and DBP (donor). BCP and MoO_3 are the electron- and hole-transporting layers, respectively. In the study of the latter cell, we simulate the possibility that C_{70} and DBP would be replaced by equivalent molecules, C_{70}^* and DBP*, with identical complex refractive indexes and bulk diffusion lengths, but a variable radiative quantum efficiency q. For this cell, the refractive indexes do not yield an increase of η with q. However, the optimal BCP and MoO_3 thicknesses do vary substantially with q.

In our computation of $\Gamma(z,q)$, we assume that radiative excitons emit at 900 nm. Furthermore, the distribution $g(z,\lambda,\theta)$ in Eq. (15) is computed by assuming that the incoming field is an even combination of TE and TM waves at oblique incidence. Finally, we assume the same value of q for the two active materials.

A. First example: High-efficiency cell

We first consider a favorable set of refractive indexes for increasing the diffusion length through the management of radiative losses. This set, together with layer thicknesses, is given in Table I. All refractive indexes are assumed independent of wavelength, except the imaginary part in the active layers, which is nonzero between 300 and 700 nm only. The assumed values of the refractive indexes for the blocking layers are consistent with the literature [29,36,52] and with the index of BCP. The large index in the active region is chosen to maximize the contrast between the blocking and photoactive layers, in accordance with the conclusion of Ref. [18]. A larger ratio of the real part of the refractive index in the photoactive layers and the blocking layers is liable to improve the cell efficiency. Furthermore, we assume an exciton diffusion length of 10 nm in both the donor and the acceptor layer, while the thickness of these layers is chosen to be 1.5 times the diffusion length. The ITO thickness of 150 nm is chosen so as to promote good light injection in the active layers thanks to constructive interferences in the spectral range of

TABLE I. Optical parameters for an example cell. The imaginary part of the refractive index in the acceptor and the donor layer is nonzero only for $\lambda \in [300, 700\text{ nm}]$.

Layer	Thickness	Refractive index	Diffusion length
Glass	∞	1.45	
ITO	150 nm	$1.76 + 0.08i$	
EBL	h_t	1.7	
Donor	15 nm	$2.8 + 0.85i$	10 nm
Acceptor	15 nm	$2.8 + 0.85i$	10 nm
HBL	h_b	1.7	
Ag	∞	$0.03 + 5.19i$	

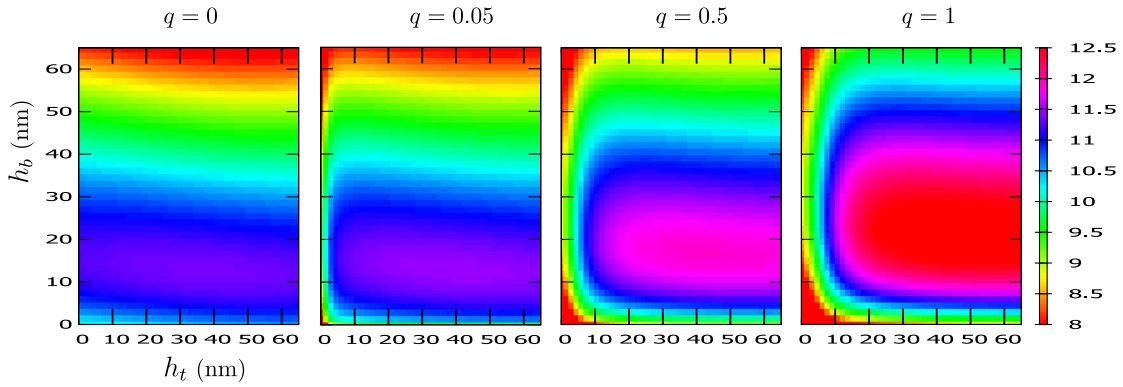

FIG. 1. Power-conversion efficiency η for the configuration presented in Table I as a function of the blocking-layer thicknesses h_t and h_b, for $q = 0$, 0.05, 0.5, 1 in both acceptor and donor layers.

interest. To avoid spurious resonances in the glass capping, we assume this layer to have infinite thickness and correct the incoming intensity accordingly.

Figure 1 shows the cell efficiency as a function of the top and bottom blocking-layer thicknesses, h_t and h_b, for three values of q. One notices that there is a qualitative change in the graph as soon as $q > 0$, with low efficiency for very small values of either h_t or h_b. This result is due to the quenching effect experienced by radiative excitons in the vicinity of a dissipative medium. As q progresses from $q = 0$ to $q = 1$, the optimal geometry varies from $(h_t, h_b) = (40, 12\ \text{nm})$ to $(h_t, h_b) = (45, 21\ \text{nm})$. Meanwhile, the cell efficiency steadily progresses from 11.3% to 12.7%; see Fig. 2. For the most efficient configuration, we plot in Fig. 3, the space-dependent decay rate $\Gamma(z, q)$ for different values of q. In that figure, the advantage of managing the exciton radiative decay is clear.

B. Second example: Low-efficiency cell

In this second example, we study the following cell, Al/BCP(h_b)/C_{70}^*(31.5 nm)/DBP*(10.5 nm)/MoO_3(h_t)/ITO(150 nm)/glass, where C_{70}^* and DBP* designate materials with identical complex refractive indexes to those of C_{70} and DBP, but where q is a free parameter. According to Ref. [53], the diffusion length is 21 nm in C_{70} and 7 nm in DBP. As in the previous example, the C_{70}^* and DBP* thicknesses are chosen to be equal to 1.5 times the diffusion length, which is consistent with Ref. [54].

The graph of η as a function of h_b and h_t is given in Fig. 4 for four values of q. This time, the maximum efficiency, 10.8%, is obtained for $q = 0$. The cell performance steadily degrades with an increasing q and does not exceed 10% for $q = 1$. However, it is important to note that the optimal configuration varies significantly between these extreme cases: For $q = 0$, the best set is near $(h_b, h_t) = (25, 0\ \text{nm})$; next, for $q = 0.05$, the optimal configuration is $(h_b, h_t) = (25, 9\ \text{nm})$; for $q = 0.5$, the optimal configuration is $(h_b, h_t) = (29, 15\ \text{nm})$; finally, for $q = 1$, it becomes $(h_b, h_t) = (32, 18\ \text{nm})$.

This last observation is a warning sign that the cell architecture should be designed with a proper account of q.

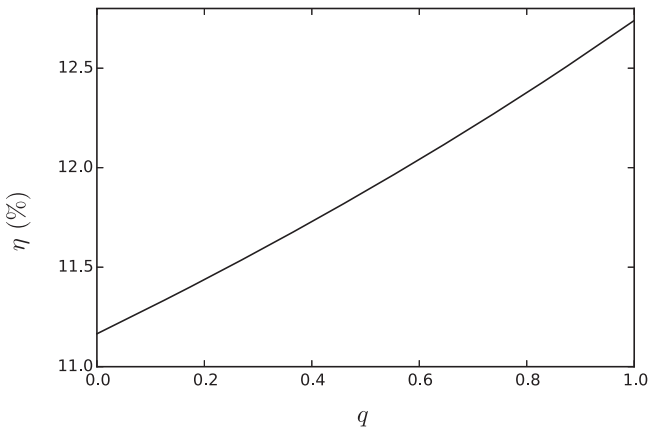

FIG. 2. Power-conversion efficiency η as a function of radiative quantum efficiency q for the parameters given in Table I and $(h_t, h_b) = (45, 21\ \text{nm})$.

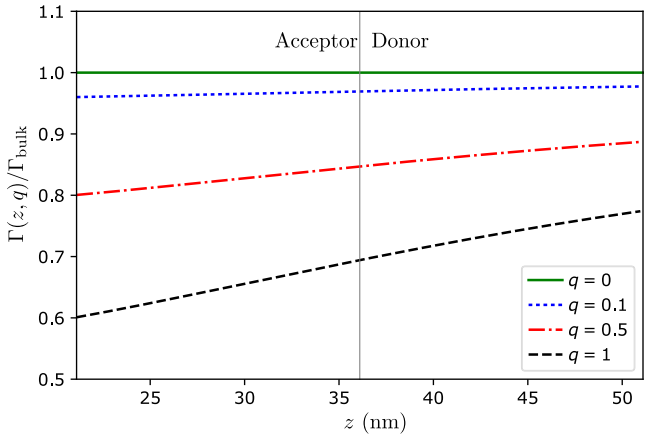

FIG. 3. Normalized exciton decay rate as a function of the distance from the back electrode for the configuration presented in Table I with $(h_t, h_b) = (45, 21\ \text{nm})$. The vertical line separates the donor and acceptor layers.

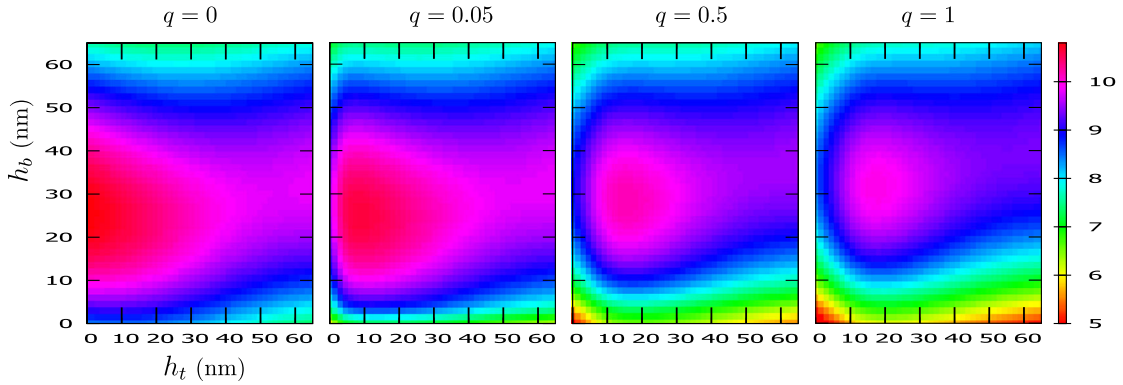

FIG. 4. Power-conversion efficiency η for Al/BCP(h_b)/C_{70}^*(31.5 nm)/DBP*(10.5 nm)/MoO_3(h_t)/ITO(150 nm)/glass as a function of h_t and h_b for $q = 0$, 0.05, 0.5, 1 in both the acceptor and donor layers.

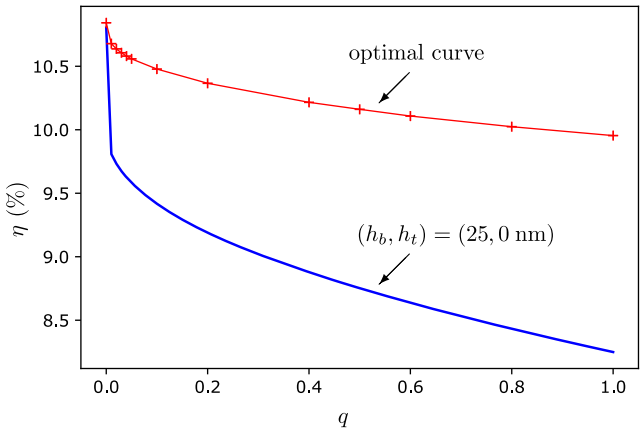

FIG. 5. Power-conversion efficiency η as a function of radiative quantum efficiency q, for Al/BCP(h_b)/C_{70}^*(31.5 nm)/DBP*(10.5 nm)/MoO_3(h_t)/ITO(150 nm)/glass cell. Blue curve, $(h_b, h_t) = (25, 0$ nm) for all q's; red curve, (h_b, h_t) set to the optimal value for each q.

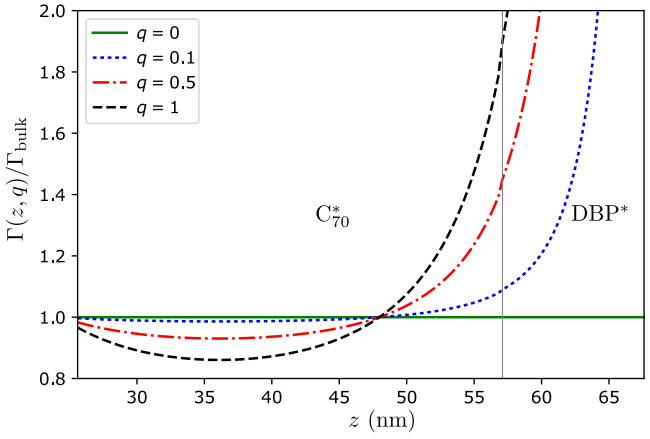

FIG. 6. Normalized exciton decay rate in the active layers for different values of q for the following configuration: Al/BCP(25 nm)/C_{70}^*(31.5 nm)/DBP*(10.5 nm)/MoO_3(0 nm)/ITO(150 nm)/glass. The vertical line separates the two active layers.

Indeed, with $(h_b, h_t) = (25, 0$ nm), which is optimal for $q = 0$; η drops from 10.8% to 8.7% if $q = 0.5$ and is only 8.2% for $q = 1$ (see Fig. 5). The cause of this rapid decay can be understood from Fig. 6, which shows $\Gamma(z, q)$ for this configuration and various values of q. Here, boundary effects strongly increase the radiative losses in DBP*. While a reduction of radiative losses is achieved in C_{70}^*, this reduction is not sufficient to counterbalance the adverse effect in DBP.

Looking again at Fig. 5, it is important to note that there is a sudden drop of η as soon as q differs from zero, even if one keeps track of the best possible configuration (h_b, h_t) while varying q. Hence, to model the organic cell with $q = 0$ is an inaccurate modeling assumption.

IV. DISCUSSION

In this paper, we emphasize the importance of properly taking into account the space-dependent rate of radiative decay of excitons, $\Gamma(z, q)$ in organic solar cells. It is well known that, as soon as the radiative quantum yield q is not zero, the radiative decay rate diverges as an exciton comes into contact with a dissipative surface [22], leading to exciton quenching. However, it has thus far been overlooked that radiative decay can be reduced elsewhere in the cell. Here, we show that with a proper choice of spacer thicknesses, h_b and h_t, this effect leads to a significant increase of the diffusion length and, hence, of the cell efficiency η. A general rule to exploit this effect is that the (real part of) the refractive-index contrast between the photoactive layers and the electron- and hole-blocking layers should be large. With a ratio of 2.8/1.7 and random exciton orientation, we numerically demonstrate an increase of η from 11.3% in the best configuration for $q = 0$ to 12.7% in the best configuration for $q = 1$. Note that the gain in efficiency rapidly increases with the refractive index in the active layers. If we suppose, for instance, that the blocking layers have a refractive index of only 1.45, then the maximum efficiency would increase from 11.3% with $q = 0$ to 14.3% with $q = 1$. Conversely, one

may seek active materials with larger refractive indexes. As an example, phthalocyanine (Pc) and its derivatives (sub-Pc, fluorinated-Pc, Mg-Pc, etc.), or subnaphthalocyanine (sub-Nc) can display refractive indexes above 3 and a large radiative quantum yield [55–60]. Similarly, perovskites are found to display large refractive indexes in their absorption range [61], along with high photoluminescence efficiency [62]. Another way to drastically improve this gain would be to orient the exciton dipole moment, preferably along the cell axis, as doing so can dramatically decrease $\Gamma(z, q)$ [18].

Based on the above calculation, it would be desirable to develop organic solar cells with molecules having a large q. In this regard, one may turn his or her attention to organic-light-emitting-device (OLED) molecules. With OLEDs, substantial development have already been made in tailoring the dipolar emission of excitons [63–65]. Moreover, q's of nearly unity and good exciton orientation have been demonstrated [66]. However, instead of maximizing exciton emission, as in OLEDs, here we want to suppress it. The maximization of η is found to require large spacers, in order both to maximize light injection and to suppress exciton decay. In practice, one is limited by the finite conductivity of these spacers. Nevertheless, large spacer values have been used in OLEDs [65] and have also been considered previously in organic solar cells [31,34,36,67,68].

It has been claimed that a good solar cell must also be a good emitter [69]. Our conclusion above that solar cells can be improved based on good exciton radiative properties is consistent with this statement. However, it should be stressed that having a large value of q is not sufficient in itself to improve the cell efficiency. We demonstrate this fact in our second numerical example. For refractive indexes corresponding to $Al/BCP/C_{70}/DBP/MoO_3/ITO/glass$, a large value of q tends to degrade the cell performance, because radiative exciton decay is increased overall in the optimal configuration. Still, taking q into account appears to be crucial. Indeed, if not properly managed, radiative losses can be worse than anticipated. Thus, even in such a case, q is an important parameter to take into account.

ACKNOWLEDGMENTS

We thank Jordi Martorell and Marina Mariano Juste (ICFO, The Institute of Photonic Sciences) for the helpful discussions and for communicating their experimental data, which were used in Sec. III B. G. K. received a Research Associateship from the Fonds de la Recherche Scientifique (FNRS), Belgium.

[1] C. W. Tang, Two-layer organic photovoltaic cell, Appl. Phys. Lett. **48**, 183 (1986).

[2] Sung Heum Park, Anshuman Roy, Serge Beaupré, Shinuk Cho, Nelson Coates, Ji Sun Moon, Daniel Moses, Mario Leclerc, Kwanghee Lee, and Alan J. Heeger, Bulk heterojunction solar cells with internal quantum efficiency approaching 100%, Nat. Photonics **3**, 297 (2009).

[3] Tayebeh Ameri, Gilles Dennler, Christoph Lungenschmied, and Christoph J. Brabec, Organic tandem solar cells: A review, Energy Environ. Sci. **2**, 347 (2009).

[4] Kjell Cnops, Barry P. Rand, David Cheyns, Bregt Verreet, Max A. Empl, and Paul Heremans, 8.4% efficient fullerene-free organic solar cells exploiting long-range exciton energy transfer, Nat. Commun. **5**, 3406 (2014).

[5] S. R. Forrest, The limits to organic photovoltaic cell efficiency, MRS Bull. **30**, 28 (2005).

[6] Bernard Kippelen and Jean-Luc Bredas, Organic photovoltaics, Energy Environ. Sci. **2**, 251 (2009).

[7] Oleksandr V. Mikhnenko, Paul W. M. Blom, and Thuc-Quyen Nguyen, Exciton diffusion in organic semiconductors, Energy Environ. Sci. **8**, 1867 (2015).

[8] Eli Yablonovitch, Statistical ray optics, J. Opt. Soc. Am. **72**, 899 (1982).

[9] Doo-Hyun Ko, John R. Tumbleston, Lei Zhang, Stuart Williams, Joseph M. DeSimone, Rene Lopez, and Edward T. Samulski, Photonic crystal geometry for organic solar cells, Nano Lett. **9**, 2742 (2009).

[10] Yingchi Liu, Christoph Kirsch, Abay Gadisa, Mukti Aryal, Sorin Mitran, Edward T. Samulski, and Rene Lopez, Effects of nano-patterned versus simple flat active layers in upright organic photovoltaic devices, J. Phys. D **46**, 024008 (2013).

[11] Yu-Sheng Hsiao, Fan-Ching Chien, Jen-Hsien Huang, Chih-Ping Chen, Chiung-Wen Kuo, Chih-Wei Chu, and Peilin Chen, Facile transfer method for fabricating light-harvesting systems for polymer solar cells, J. Phys. Chem. C **115**, 11864 (2011).

[12] Jonathan Grandidier, Dennis M. Callahan, Jeremy N. Munday, and Harry A. Atwater, Light absorption enhancement in thin-film solar cells using whispering gallery modes in dielectric nanospheres, Adv. Mater. **23**, 1272 (2011).

[13] Yan Yao, Jie Yao, Vijay Kris Narasimhan, Zhichao Ruan, Chong Xie, Shanhui Fan, and Yi Cui, Broadband light management using low-q whispering gallery modes in spherical nanoshells, Nat. Commun. **3**, 664 (2012).

[14] Marina Mariano, Francisco J. Rodríguez, Pablo Romero-Gomez, Gregory Kozyreff, and Jordi Martorell, Light coupling into the whispering gallery modes of a fiber array thin film solar cell for fixed partial sun tracking, Sci. Rep. **4**, 4959 (2014).

[15] Marina Mariano, Gregory Kozyreff, Luis G. Gerling, Pablo Romero-Gomez, Joaquim Puigdollers, Jorge Bravo-Abad, and Jordi Martorell, Intermittent chaos for ergodic light trapping in a photonic fiber plate, Light Sci. Appl. **5**, e16216 (2016).

[16] Thomas Kirchartz, Kurt Taretto, and Uwe Rau, Efficiency limits of organic bulk heterojunction solar cells, J. Phys. Chem. C **113**, 17958 (2009).

[17] Dirk Veldman, Özlem Ipek, Stefan C. J. Meskers, Jörgen Sweelssen, Marc M. Koetse, Sjoerd C. Veenstra, Jan M. Kroon, Svetlana S. van Bavel, Joachim Loos, and René A. J. Janssen, Compositional and electric field dependence of the dissociation of charge transfer excitons in alternating polyfluorene copolymer/fullerene blends, J. Am. Chem. Soc. **130**, 7721 (2008).

[18] G. Kozyreff, D. C. Urbanek, L. T. Vuong, O. Nieto Silleras, and J. Martorell, Microcavity effects on the generation, fluorescence, and diffusion of excitons in organic solar cells, Opt. Express **21**, A336 (2013).
[19] K. H. Drexhage, in *Progress in Optics*, Vol. 12, edited by E. Wolf (Elsevier, New York, 1974), p. 163.
[20] A. Sommerfeld, Propagation of waves in wireless telegraphy, Ann. Phys. (Berlin) **333**, 665 (1909).
[21] A. Sommerfeld, *Partial Differential Equations in Physics* (Academic Press, New York, 1949).
[22] R. R. Chance, A. Prock, and R. Silbey, Molecular fluorescence and energy transfer near interfaces, Adv. Chem. Phys. **37**, 1 (1978).
[23] W. Lukosz, Theory of optical-environment-dependent spontaneous-emission rates for emitters in thin layers, Phys. Rev. B **22**, 3030 (1980).
[24] K. A. Neyts, Simulation of light emission from thin-film microcavities, J. Opt. Soc. Am. A **15**, 962 (1998).
[25] J. A. E. Wasey, A. Safonov, I. D. W. Samuel, and W. L. Barnes, Effects of dipole orientation and birefringence on the optical emission from thin films, Opt. Commun. **183**, 109 (2000).
[26] T. Tsutsui, C. Adachi, S. Saito, M. Watanabe, and M. Koishi, Effect of confined radiation field on spontaneous-emission lifetime in vacuum-deposited fluorescent dye films, Chem. Phys. Lett. **182**, 143 (1991).
[27] R. M. Amos and W. L. Barnes, Modification of the spontaneous emission rate of Eu^{3+} ions close to a thin metal mirror, Phys. Rev. B **55**, 7249 (1997).
[28] Daniel Kleppner, Inhibited Spontaneous Emission, Phys. Rev. Lett. **47**, 233 (1981).
[29] Peter Peumans, Aharon Yakimov, and Stephen R. Forrest, Small molecular weight organic thin-film photodetectors and solar cells, J. Appl. Phys. **93**, 3693 (2003).
[30] Seunghyup Yoo, William J. Potscavage, Jr., Benoit Domercq, Sung-Ho Han, Tai-De Li, Simon C. Jones, Robert Szoszkiewicz, Dean Levi, Elisa Riedo, Seth R. Marder, and Bernard Kippelen, Analysis of improved photovoltaic properties of pentacene/C_{60} organic solar cells: Effects of exciton blocking layer thickness and thermal annealing, Solid State Electron. **51**, 1367 (2007).
[31] Jane Lee, Sei-Yong Kim, Changsoon Kim, and Jang-Joo Kim, Enhancement of the short circuit current in organic photovoltaic devices with microcavity structures, Appl. Phys. Lett. **97**, 083306 (2010).
[32] Yongbing Long, Improving optical performance of low bandgap polymer solar cells by the two-mode moderate microcavity, Appl. Phys. Lett. **98**, 033301 (2011).
[33] Yongbing Long, Red and near-infrared absorption enhancement for low bandgap polymer solar cells by combining the optical microcavity and optical spacers, Sol. Energy Mater. Sol. Cells **95**, 3400 (2011).
[34] Rafael Betancur, Alberto Martínez-Otero, Xavier Elias, Pablo Romero-Gómez, Silvia Colodrero, Hernán Miguez, and Jordi Martorell, Optical interference for the matching of the external and internal quantum efficiencies in organic photovoltaic cells, Sol. Energy Mater. Sol. Cells **104**, 87 (2012).
[35] José-Francisco Salinas, Hin-Lap Yip, Chu-Chen Chueh, Chang-Zhi Li, José-Luis Maldonado, and Alex K.-Y. Jen, Optical design of transparent thin metal electrodes to enhance in-coupling and trapping of light in flexible polymer solar cells, Adv. Mater. **24**, 6362 (2012).
[36] Kung-Shih Chen, Hin-Lap Yip, José-Francisco Salinas, Yun-Xiang Xu, Chu-Chen Chueh, and Alex K.-Y. Jen, Strong photocurrent enhancements in highly efficient flexible organic solar cells by adopting a microcavity configuration, Adv. Mater. **26**, 3349 (2014).
[37] Chu-Chen Chueh, Michael Crump, and Alex K.-Y. Jen, Optical enhancement via electrode designs for high-performance polymer solar cells, Adv. Funct. Mater. **26**, 321 (2016).
[38] William Shockley and Hans J. Queisser, Detailed balance limit of efficiency of *p-n* junction solar cells, J. Appl. Phys. **32**, 510 (1961).
[39] P. Würfel, The chemical potential of radiation, J. Phys. C **15**, 3967 (1982).
[40] J. Nelson, *The Physics of Solar Cells* (Imperial College Press, London, 2003).
[41] A. De Vos, *Thermodynamics of Solar Energy Conversion* (Wiley-VCH, Weinheim, 2008).
[42] Seunghyup Yoo, Benoit Domercq, and Bernard Kippelen, Efficient thin-film organic solar cells based on pentacene/C_{60} heterojunctions, Appl. Phys. Lett. **85**, 5427 (2004).
[43] Thomas Kirchartz, Jenny Nelson, and Uwe Rau, Reciprocity between Charge Injection and Extraction and Its Influence on the Interpretation of Electroluminescence Spectra in Organic Solar Cells, Phys. Rev. Applied **5**, 054003 (2016).
[44] Koen Vandewal, Zaifei Ma, Jonas Bergqvist, Zheng Tang, Ergang Wang, Patrik Henriksson, Kristofer Tvingstedt, Mats R. Andersson, Fengling Zhang, and Olle Ingans, Quantification of quantum efficiency and energy losses in low bandgap polymer:fullerene solar cells with high open-circuit voltage, Adv. Funct. Mater. **22**, 3480 (2012).
[45] Uwe Rau, Reciprocity relation between photovoltaic quantum efficiency and electroluminescent emission of solar cells, Phys. Rev. B **76**, 085303 (2007).
[46] Uwe Rau, Beatrix Blank, Thomas C. M. Müller, and Thomas Kirchartz, Efficiency Potential of Photovoltaic Materials and Devices Unveiled by Detailed-Balance Analysis, Phys. Rev. Applied **7**, 044016 (2017).
[47] M. Born and E. Wolf, *Principle of Optics* (Pergamon, New York, 1991).
[48] Leif A. A. Pettersson, Lucimara S. Roman, and Olle Inganäs, Modeling photocurrent action spectra of photovoltaic devices based on organic thin films, J. Appl. Phys. **86**, 487 (1999).
[49] S. R. Scully and M. D. McGehee, Effects of optical interference and energy transfer on exciton diffusion length measurements in organic semiconductors, J. Appl. Phys. **100**, 034907 (2006).
[50] Thomas Stübinger and Wolfgang Brütting, Exciton diffusion and optical interference in organic donor-acceptor photovoltaic cells, J. Appl. Phys. **90**, 3632 (2001).
[51] Jiang Huang, Chang-Zhi Li, Chu-Chen Chueh, Sheng-Qiang Liu, Jun-Sheng Yu, and Alex K.-Y. Jen, 10.4% power conversion efficiency of ITO-free organic photovoltaics through enhanced light trapping configuration, Adv. Energy Mater. **5**, 1500406 (2015).

[52] B. P. Rand, D. P. Burk, and S. R. Forrest, Offset energies at organic semiconductor heterojunction and their influence on the open-circuit voltage of thin-film solar cells, Phys. Rev. B **75**, 115327 (2007).

[53] Daisuke Yokoyama, Zhong Qiang Wang, Yong-Jin Pu, Kenta Kobayashi, Junji Kido, and Ziruo Hong, High-efficiency simple planar heterojunction organic thin-film photovoltaics with horizontally oriented amorphous donors, Sol. Energy Mater. Sol. Cells **98**, 472 (2012).

[54] Bernhard Siegmund, Muhammad T. Sajjad, Johannes Widmer, Debdutta Ray, Christian Koerner, Moritz Riede, Karl Leo, Ifor D. W. Samuel, and Koen Vandewal, Exciton diffusion length and charge extraction yield in organic bilayer solar cells, Adv. Mater. **29**, 1604424 (2017).

[55] H. H. P. Gommans, D. Cheyns, T. Aernouts, C. Girotto, J. Poortmans, and P. Heremans, Electro-optical study of subphthalocyanine in a bilayer organic solar cell, Adv. Funct. Mater. **17**, 2653 (2007).

[56] Michał Wojdyła, Wacław Bała, Beata Derkowska, Mateusz Rebarz, and Andrzej Korcala, The temperature dependence of photoluminescence and absorption spectra of vacuum-sublimed magnesium phthalocyanine thin films, Opt. Mater. **30**, 734 (2008).

[57] Richard R. Lunt, Noel C. Giebink, Anna A. Belak, Jay B. Benziger, and Stephen R. Forrest, Exciton diffusion lengths of organic semiconductor thin films measured by spectrally resolved photoluminescence quenching, J. Appl. Phys. **105**, 053711 (2009).

[58] Bregt Verreet, Sarah Schols, David Cheyns, Barry P. Rand, Hans Gommans, Tom Aernouts, Paul Heremans, and Jan Genoe, The characterization of chloroboron (III) subnaphthalocyanine thin films and their application as a donor material for organic solar cells, J. Mater. Chem. **19**, 5295 (2009).

[59] Bregt Verreet, Barry P. Rand, David Cheyns, Afshin Hadipour, Tom Aernouts, Paul Heremans, Anas Medina, Christian G. Claessens, and Tomas Torres, A 4% efficient organic solar cell using a fluorinated fused subphthalocyanine dimer as an electron acceptor, Adv. Energy Mater. **1**, 565 (2011).

[60] S. Matthew Menke, Wade A. Luhman, and Russell J. Holmes, Tailored exciton diffusion in organic photovoltaic cells for enhanced power conversion efficiency, Nat. Mater. **12**, 152 (2013).

[61] Qianqian Lin, Ardalan Armin, Ravi Chandra Raju Nagiri, Paul L. Burn, and Paul Meredith, Electro-optics of perovskite solar cells, Nat. Photonics **9**, 106 (2015).

[62] Felix Deschler, Michael Price, Sandeep Pathak, Lina E. Klintberg, David-Dominik Jarausch, Ruben Higler, Sven Httner, Tomas Leijtens, Samuel D. Stranks, Henry J. Snaith *et al.*, High photoluminescence efficiency and optically pumped lasing in solution-processed mixed halide perovskite semiconductors, J. Phys. Chem. Lett. **5**, 1421 (2014).

[63] Michael Flämmich, Malte C. Gather, Norbert Danz, Dirk Michaelis, and Klaus Meerholz, In situ measurement of the internal luminescence quantum efficiency in organic light-emitting diodes, Appl. Phys. Lett. **95**, 263306 (2009).

[64] Michael Flämmich, Malte C. Gather, Norbert Danz, Dirk Michaelis, Andreas H. Bräuer, Klaus Meerholz, and Andreas Tünnermann, Orientation of emissive dipoles in ODEDs: Quantitative in situ analysis, Org. Electron. **11**, 1039 (2010).

[65] L. Penninck, F. Steinbacher, R. Krause, and K. Neyts, Determining emissive dipole orientation in organic light emitting devices by decay time measurement, Org. Electron. **13**, 3079 (2012).

[66] Sei-Yong Kim, Won-Ik Jeong, Christian Mayr, Young-Seo Park, Kwon-Hyeon Kim, Jeong-Hwan Lee, Chang-Ki Moon, Wolfgang Brütting, and Jang-Joo Kim, Organic light-emitting diodes with 30% external quantum efficiency based on a horizontally oriented emitter, Adv. Funct. Mater. **23**, 3896 (2013).

[67] Brian E. Lassiter, Guodan Wei, Siyi Wang, Jeramy D. Zimmerman, Viacheslav V. Diev, Mark E. Thompson, and Stephen R. Forrest, Organic photovoltaics incorporating electron conducting exciton blocking layers, Appl. Phys. Lett. **98**, 243307 (2011).

[68] M. Z. Sahdan, M. F. Malek, M. S. Alias, S. A. Kamaruddin, C. A. Norhidayah, N. Sarip, N. Nafarizal, and M. Rusop, Metamorphosis of the ZnO buffer layer thicknesses on the performance of inverted organic solar cells, J. Mater. Sci. Mater. Electron. **27**, 12891 (2016).

[69] O. D. Miller, E. Yablonovitch, and S. R. Kurtz, Strong internal and external luminescence as solar cells approach the Shockley-Queisser limits, IEEE J. Photovoltaics **2**, 303 (2012).